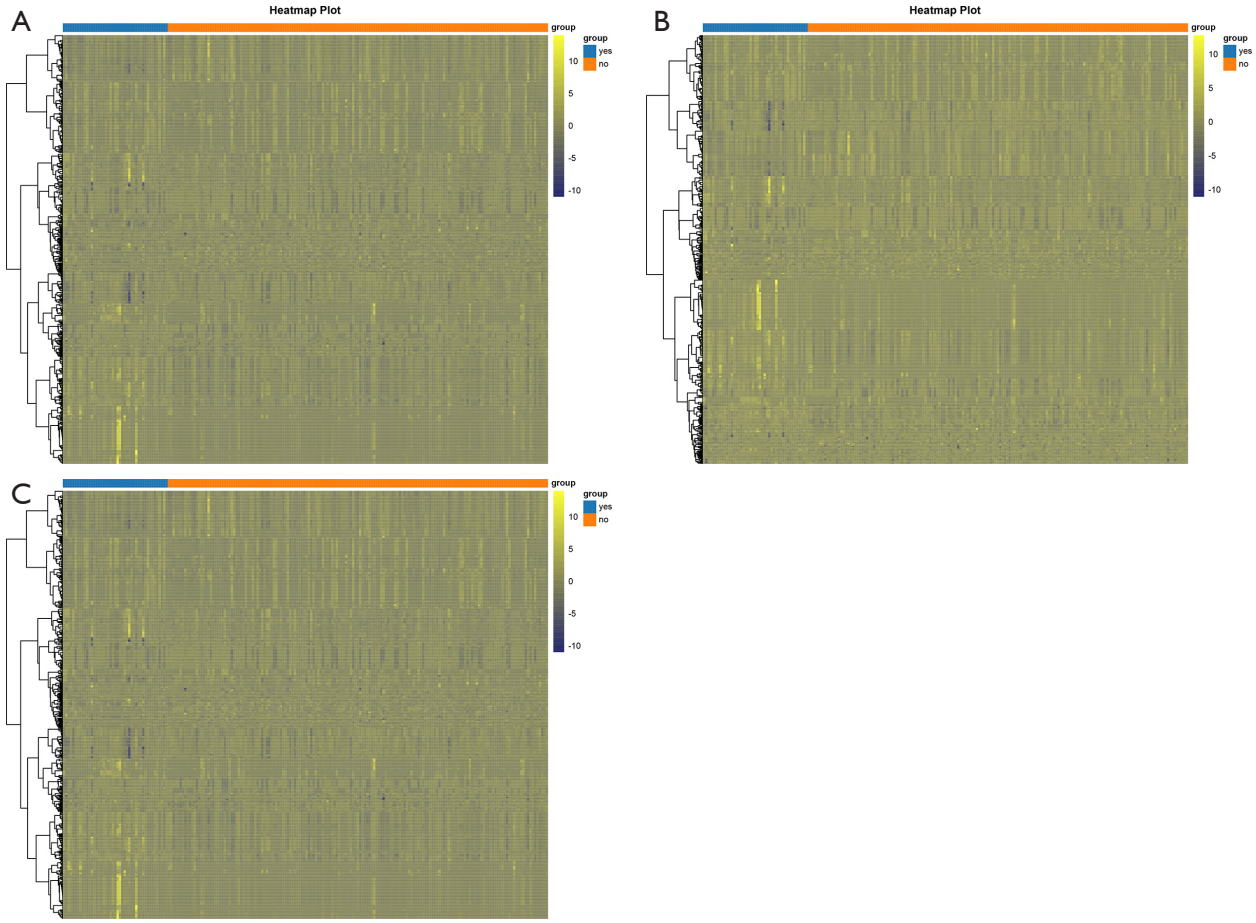

Figure S1 Heatmap of the full radiomic features. (A) Heatmap for 3-mm peritumoral features. (B) Heatmap for 5-mm peritumoral features. (C) Heatmap for intratumoral features.

© AME Publishing Company.
https://dx.doi.org/10.21037/tlcr-24-565

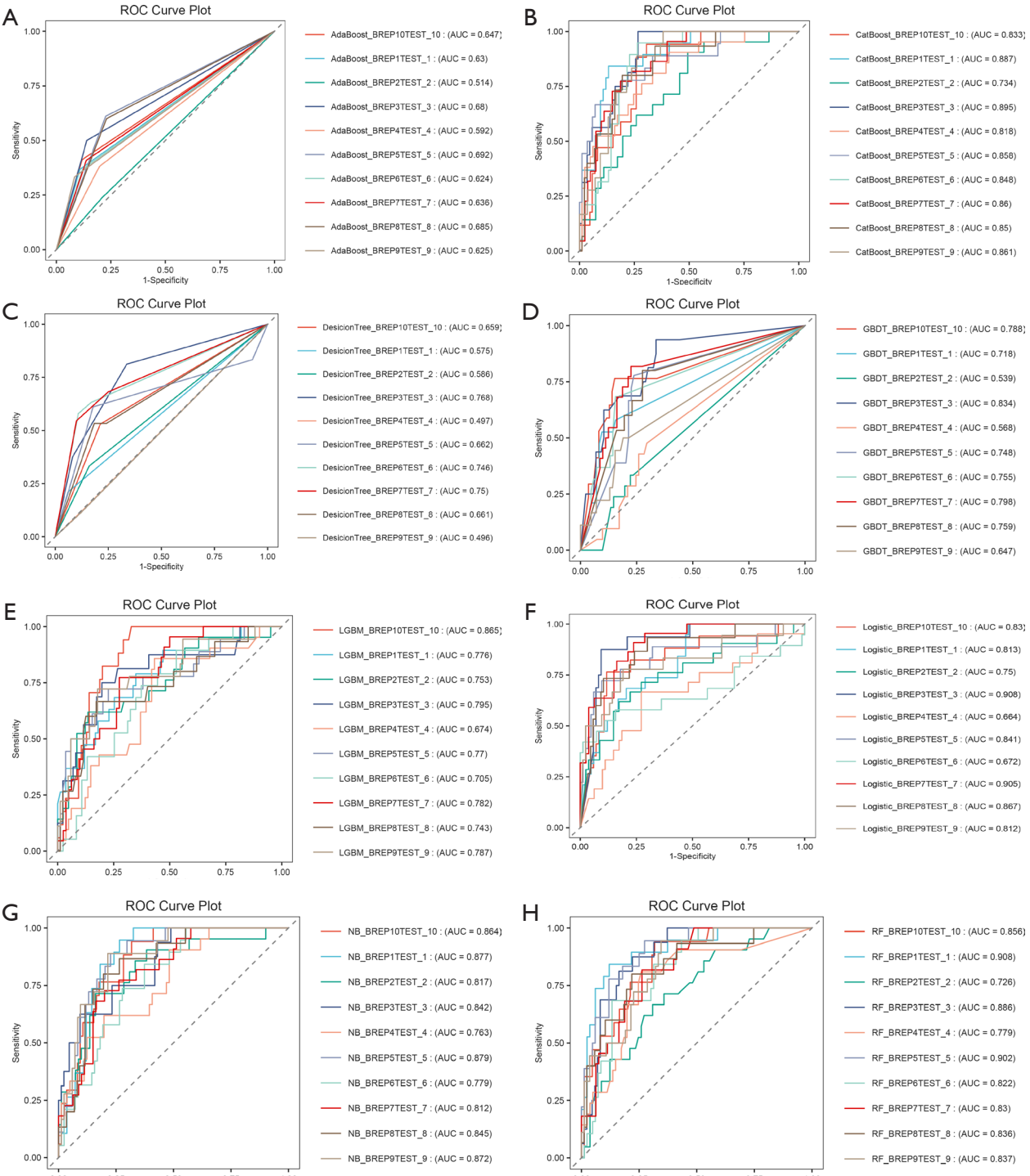

© AME Publishing Company.
https://dx.doi.org/10.21037/tlcr-24-565

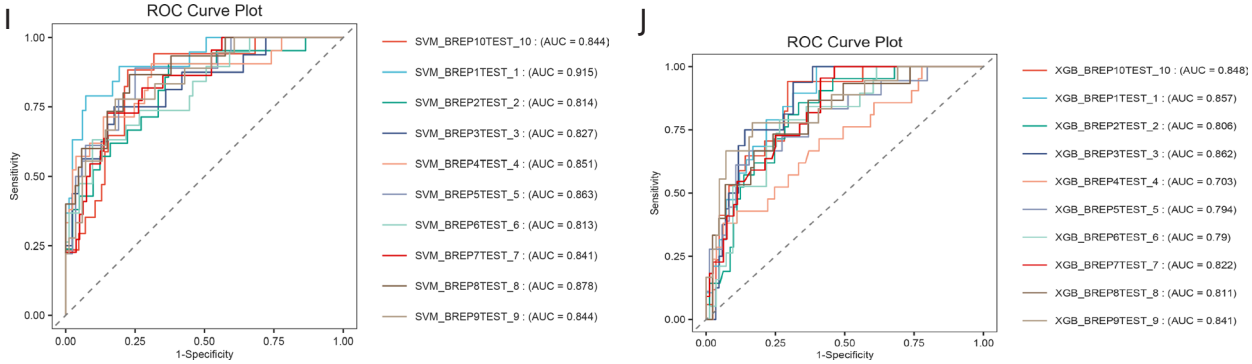

Figure S2 Comparison of 10 machine learning algorithms in the train set containing peritumour 3-mm features. (A) The ROC results of the AdaBoost model in the train set. (B) The ROC results of the CatBoost model in the train set. (C) The ROC results of the DesicionTree model in the train set. (D) The ROC results of the GBDT model in the train set. (E) The ROC results of the LGBM model in the train set. (F) The ROC results of the Logistic model in the train set. (G) The ROC results of the NB model in the train set. (H) The ROC results of the RF model in the train set. (I) The ROC results of the SVM model in the train set. (J) The ROC results of the XGB model in the train set. ROC, receiver operating characteristic; AUC, area under the curve; AdaBoost, Adaptive Boosting; CatBoost, Categorical Boosting; GBDT, Gradient Boosting Decision Tree; LGBM, Light Gradient Boosting Machine; NB, Naive Bayes; RF, Random Forest; SVM, Support Vector Machines; XGB, eXtreme Gradient Boosting.

© AME Publishing Company.
https://dx.doi.org/10.21037/tlcr-24-565

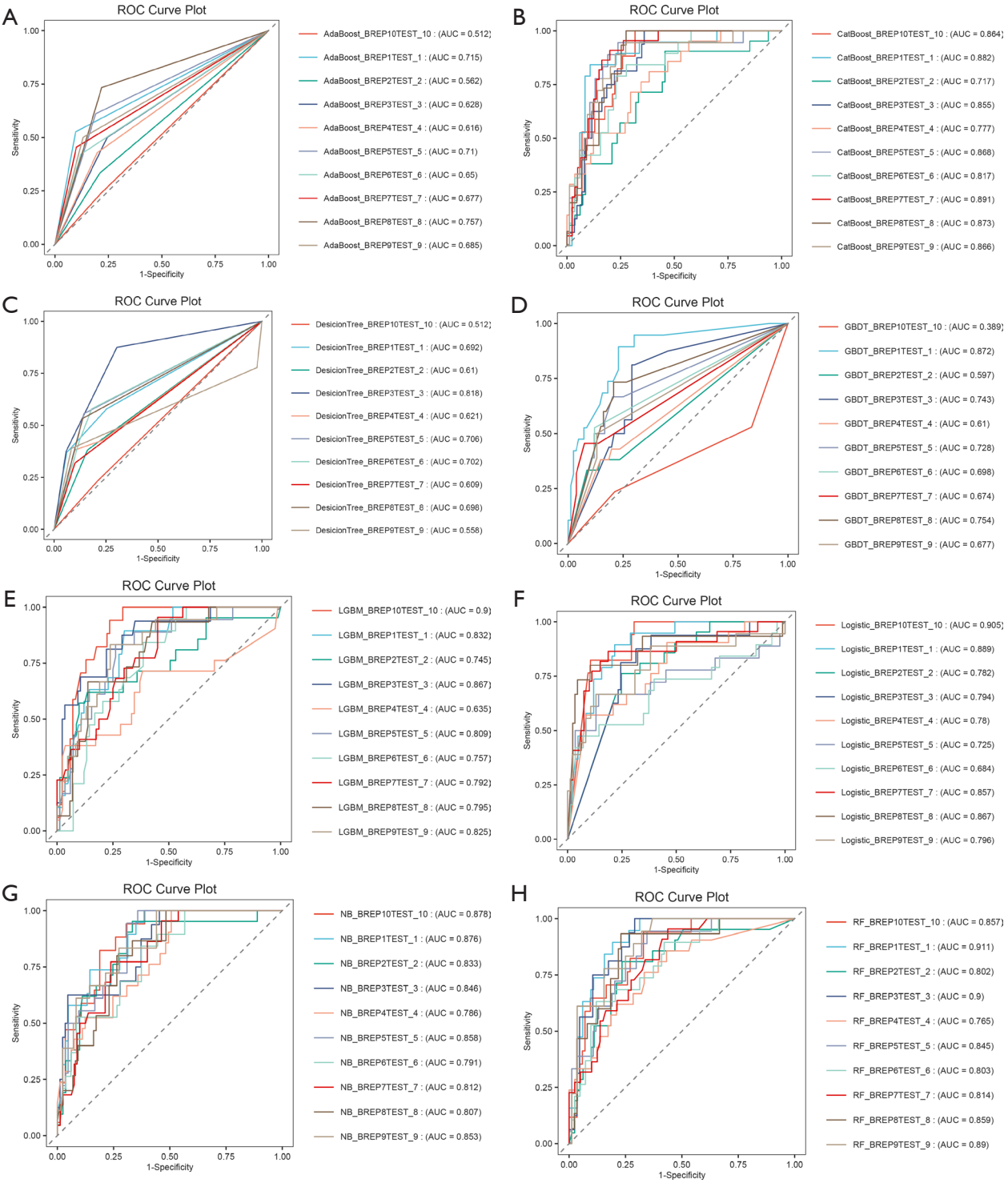

© AME Publishing Company.
https://dx.doi.org/10.21037/tlcr-24-565

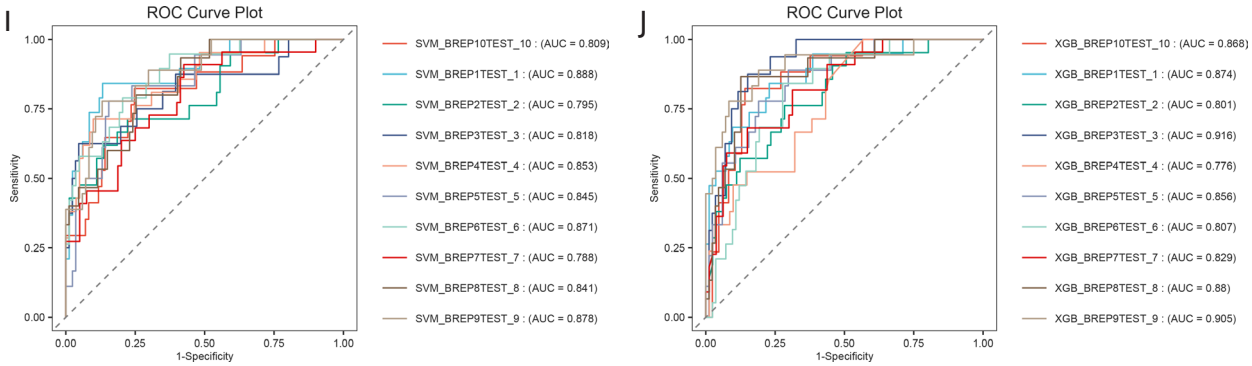

Figure S3 Comparison of 10 machine learning algorithms in the train set containing peritumour 5-mm features. (A) The ROC results of the AdaBoost model in the train set. (B) The ROC results of the CatBoost model in the train set. (C) The ROC results of the DesicionTree model in the train set. (D) The ROC results of the GBDT model in the train set. (E) The ROC results of the LGBM model in the train set. (F) The ROC results of the logistic model in the train set. (G) The ROC results of the NB model in the train set. (H) The ROC results of the RF model in the train set. (I) The ROC results of the SVM model in the train set. (J) The ROC results of the XGB model in the train set. ROC, receiver operating characteristic; AUC, area under the curve; AdaBoost, Adaptive Boosting; CatBoost, Categorical Boosting; GBDT, Gradient Boosting Decision Tree; LGBM, Light Gradient Boosting Machine; NB, Naive Bayes; RF, Random Forest; SVM, Support Vector Machines; XGB, eXtreme Gradient Boosting.

© AME Publishing Company.
https://dx.doi.org/10.21037/tlcr-24-565

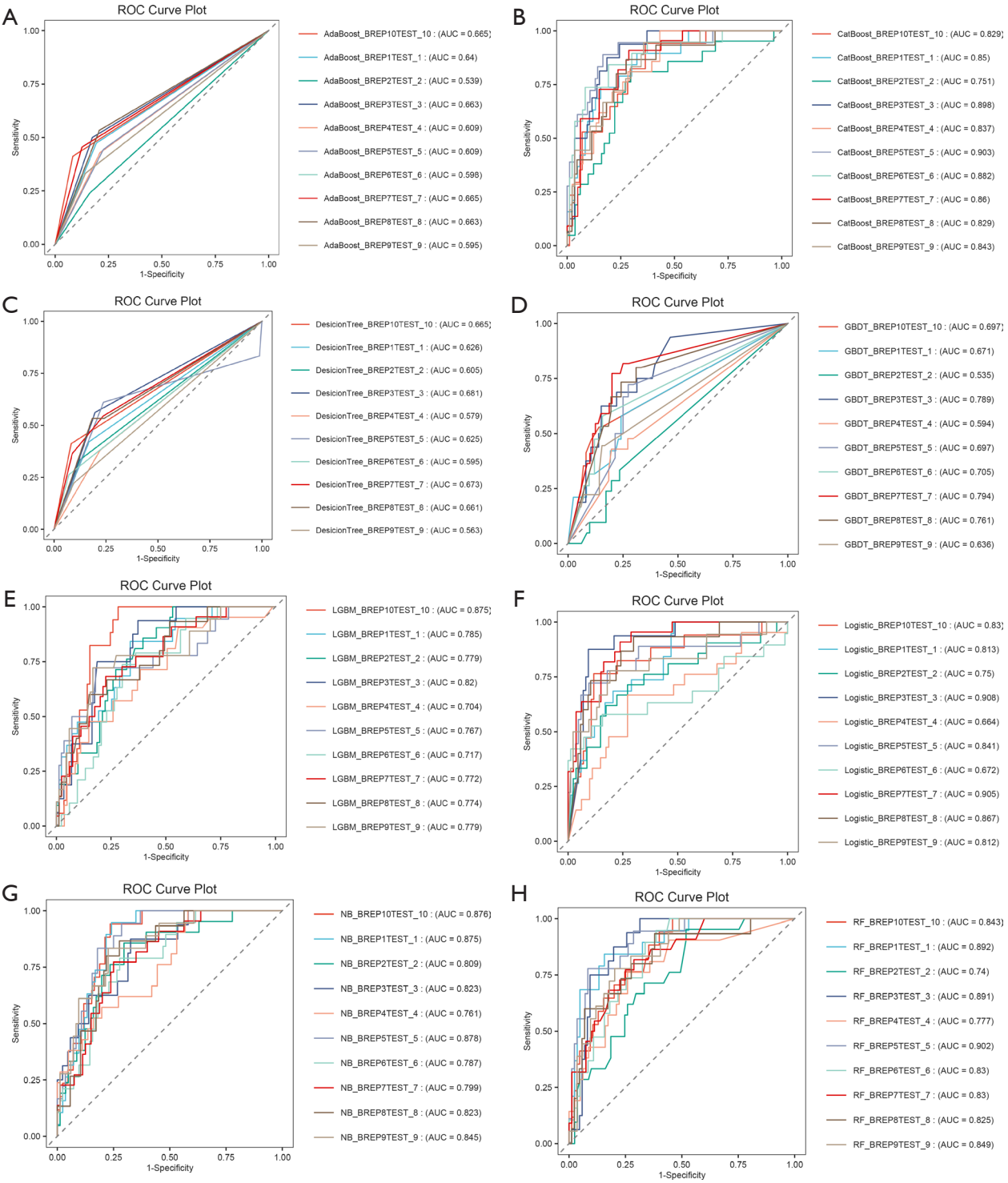

© AME Publishing Company.
https://dx.doi.org/10.21037/tlcr-24-565

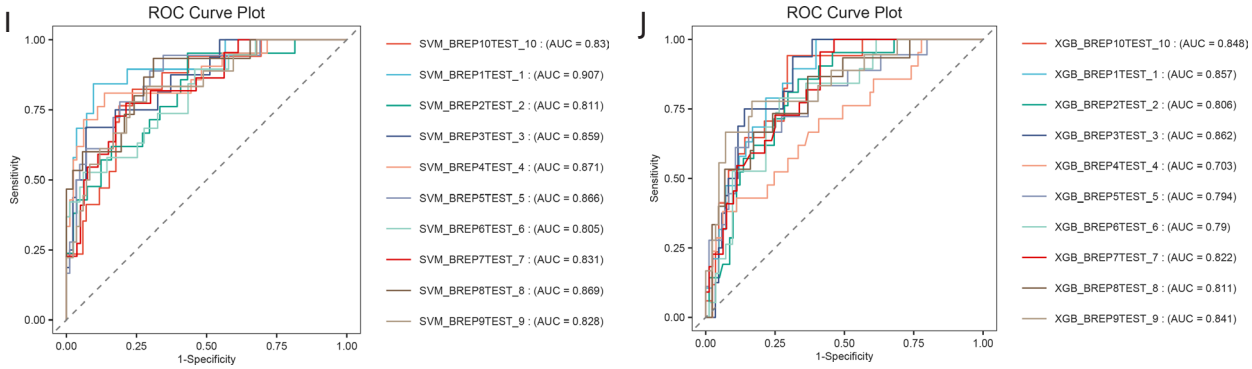

Figure S4 Comparison of 10 machine learning algorithms in the train set containing intratumoral features. (A) The ROC results of the AdaBoost model in the train set. (B) The ROC results of the CatBoost model in the train set. (C) The ROC results of the DesicionTree model in the train set. (D) The ROC results of the GBDT model in the train set. (E) The ROC results of the LGBM model in the train set. (F) The ROC results of the Logistic model in the train set. (G) The ROC results of the NB model in the train set. (H) The ROC results of the RF model in the train set. (I) The ROC results of the SVM model in the train set. (J) The ROC results of the XGB model in the train set. ROC, receiver operating characteristic; AUC, area under the curve; AdaBoost, Adaptive Boosting; CatBoost, Categorical Boosting; GBDT, Gradient Boosting Decision Tree; LGBM, Light Gradient Boosting Machine; NB, Naive Bayes; RF, Random Forest; SVM, Support Vector Machines; XGB, eXtreme Gradient Boosting.

© AME Publishing Company.
https://dx.doi.org/10.21037/tlcr-24-565

Table S1 Comparative analysis of the predictive performance of the best machine learning models in three modules

Module	Model name	Recall	Accuracy	F1-score	MCC	AUROC
Intratumoral	Train	0.929	0.959	0.897	0.872	0.992
	Test	0.471	0.762	0.516	0.363	0.818
	Validation	0.651	0.763	0.727	0.603	0.873
	Mean	0.683	0.828	0.713	0.613	0.894
3-mm peritumoral expansion	Train	0.786	0.959	0.880	0.865	0.993
	Test	0.706	0.825	0.686	0.565	0.858
	Validation	0.659	0.890	0.710	0.693	0.981
	Mean	0.717	0.891	0.758	0.708	0.944
5-mm peritumoral expansion	Train	0.714	0.945	0.833	0.818	0.984
	Test	0.353	0.714	0.400	0.220	0.838
	Validation	0.632	0.851	0.711	0.669	0.952
	Mean	0.566	0.837	0.648	0.569	0.925

MCC: Matthews Correlation Coefficient; AUROC, area under the receiver operating characteristic curve.

Table S2 The key radiomics features

Conventional radiological features	Semantics	Radiomics features
Longest diameter	Lobulation	Lung_nii_original_glszm_ZoneVariance
Size of solid components	Spiculation	Lung_nii_logarithm_glszm_ZoneVariance
CTR	Vacuole	Lung_nii_wavelet_LLH_glcm_SumEntropy
Lymph node short diameter	Pleural indentation	Lung_nii_wavelet_LHH_firstorder_Mean
	Internal vascular sign	Lung_nii_wavelet_LHH_firstorder_Skewness
	Bronchial anomaly sign	Lung_nii_wavelet_LHH_glcm_MCC
		Lung_nii_wavelet_LHH_glrlm_LongRunLowGrayLevelEmphasis
		Lung_nii_wavelet_HLL_glszm_LargeAreaLowGrayLevelEmphasis
		Lung_nii_wavelet_HHL_ngtdm_Contrast
		Lung_nii_wavelet_HHH_glszm_ZoneEntropy
		Lung_nii_wavelet_LLL_firstorder_90Percentile
		Lung_nii_wavelet_LLL_firstorder_Range
		Lung_nii_wavelet_LLL_glszm_LargeAreaEmphasis
		Lung_nii_square_firstorder_Median
		Lung_nii_square_firstorder_RobustMeanAbsoluteDeviation
		Lung_nii_lbp_3D_k_glrlm_ShortRunHighGrayLevelEmphasis

CTR, consolidation-to-tumor ratio; MCC, Matthews Correlation Coefficient; LLL, low-low-low; LHH, low-high-high; HHL, high-high-low; LLH, low-low-high; HHH, high-high-high.

© AME Publishing Company.
https://dx.doi.org/10.21037/tlcr-24-565